Available online at www.sciencedirect.com
ScienceDirect
Journal of the European Ceramic Society 28 (2008) 2411–2419
www.elsevier.com/locate/jeurceramsoc

Directional solidification of Al_2O_3–Al_2TiO_5 system

Marie-Hélène Berger[a], Ali Sayir[b,*]

[a] Centre des Matériaux, Mines Paris, ParisTech, CNRS UMR 7633, BP 87, 91003 Evry Cedex, France
[b] NASA Glenn Research Center, CWRU, MS 106, 21000 Brookpark Road, Cleveland OH 44135, USA

Available online 9 May 2008

Abstract

Directional solidification of Al_2O_3–Al_2TiO_5 eutectic system was investigated to design in situ composites that could exhibit optimized properties of strength and toughness. Directional solidification of an alumina rich melt was expected to produce primary Al_2O_3 dendrites, these would act as load bearing component of the structure, separated by a Al_2O_3–Al_2TiO_5 eutectic matrix and. Additional aim was to utilize the differential expansion coefficient between the two phases to produce microcracks and thus weak interfaces for load deflection. Three different melt compositions were investigated; two off-eutectic compositions, at 11, 26 mol% TiO_2, and one eutectic at 43.9 mol% TiO_2. The crystallized phases were different than as one would expect from the published phase diagram. Off-eutectics were composed of Al_2O_3 dendrites separated by a $Al_6Ti_2O_{13}$ matrix. Eutectic structure was composed of Al_2TiO_5 lamellae in an aluminum titanate matrix. This matrix consisted of a superstructure made of 5 cells of $Al_6Ti_2O_{13}$ for one cell of Al_2TiO_5 along [0 0 1] direction. Al_6TiO_{13} phase decomposed by a eutectoid reaction into Al_2O_3 and Al_2TiO_5. Eutectoid reaction occurred during post heat treatment at 1400 °C and decomposition of $Al_6Ti_2O_{13}$ was completed after 10 h of annealing at 1500 °C. Based on these observations, a modification of the alumina rich part of Al_2O_3–TiO_2 phase diagram was proposed. A second intermediate compound, $Al_6Ti_2O_{13}$ is introduced as a high temperature phase. Two invariant points, a peritectic ($L + Al_2O_3 \rightarrow Al_6Ti_2O_{13}$) and a eutectic ($L \rightarrow Al_6Ti_2O_{13} + Al_2TiO_5$) are also added between $Al_6Ti_2O_{13}$ and Al_2TiO_5.
© 2008 Elsevier Ltd. All rights reserved.

Keywords: Directional solidification; Electron microscopy; Al_2O_3; Al_2TiO_5

1. Introduction

Directionally solidified eutectic ceramics exhibit remarkable thermo-mechanical stability. They can retain 90% of their RT strength above 1600 °C and show outstanding creep resistance.[1–8] Their specific microstructure made of entangled two-phase single crystals hinders deformation mechanisms that usually take place in sintered ceramics. Diffusion paths are lengthened by the elongated microstructure and dislocation motion is restricted by the fine width of each phase and the coherent heterophase interfaces. These strong interfaces have little effect in deflecting or arresting crack propagation. Therefore directionally solidified eutectic ceramics show catastrophic failures and low toughness values. The objective of this work was to design an in situ composite by directional solidification that exhibits an optimized balance between strength and toughness.

The Al_2O_3–Al_2TiO_5 system was chosen for this study because of the large anisotropy in CTE of Al_2TiO_5[9,10] resulting in an anisotropic mismatch between the two phases as seen in Table 1. Al_2O_3–TiO_2 phase diagrams[11–13] indicate that Al_2TiO_5 is the unique intermediate compound and a eutectic invariant point between Al_2O_3 and Al_2TiO_5 is reported for 43.9 mol% TiO_2. Micro-cracks or weak interfaces are expected to develop in the eutectic structure upon cooling. Table 1 shows that weakest interfaces will be found for interface parallel to (1 0 0) or (0 0 1) of Al_2TiO_5 whatever the direction of Al_2O_3 is. The length of the crack in the eutectic will be restricted by the tortuous interfaces of and their orientation changes. Such a micro-cracked eutectic is expected to exhibit higher toughness but also lower strength if crack lengths exceed critical values of defect length. A balance between strength and toughness could be achieved by reinforcing the eutectic matrix by a continuous load-bearing phase with a larger strain to failure than the matrix. The examination of the Al_2O_3–TiO_2 phase diagrams shows that the directional solidification from an alumina rich off eutectic melt should produce continuous Al_2O_3 primary dendrites separated by a Al_2TiO_5/Al_2O_3 eutectic matrix. Weak interfaces are also expected to develop locally along interfaces between Al_2O_3 dendrites and the Al_2TiO_5 phase of eutectic matrix.

* Corresponding author. Tel.: +1 216 433 6254.
E-mail address: ali.sayir-1@nasa.gov (A. Sayir).

0955-2219/$ – see front matter © 2008 Elsevier Ltd. All rights reserved.
doi:10.1016/j.jeurceramsoc.2008.03.005

Table 1
CTE mismatch between Al_2O_3 and Al_2TiO_5 ($10^6\,C^{-1}$, 25–1000 °C)

	Al_2O_3 ($R\bar{3}c$)	
	$\alpha_a = 7.7$	$\alpha_c = 8.6$
Al_2TiO_5 (*Cmcm*)		
$\alpha_a = -2.7$	10.4	11.3
$\alpha_b = 10.9$	−3.2	−2.3
$\alpha_c = 20.5$	−12.8	−11.9

These characteristics should provide an in situ composite with higher strength that the eutectic matrix and a failure mode comparable with those of ceramic matrix composites. The starting objective of this work was to examine these postulations. However it came out from microstructural observations that phases formed during solidification of alumina rich and eutectic melts were not those foreseen by the phase diagrams. As a consequence, the first part of this paper will present the phases obtained from the solidification of an alumina rich and eutectic melts and their stability. The second part will discuss the validity of the existing phase diagrams, and propose a direction for their revision. Mechanical characteristics of the eutectic and off eutectics materials are presented in Refs. [14,15].

2. Experimental

The materials were processed, by the laser heated float zone method[4,7] using a pulling rate of 5–10 mm/min, in the shape of rods of about 4 mm diameter. Source material (10 mm in diameter) were fabricated by wet mixing, isostatic pressing into a rod shape and sintering (1450 °C in air). The raw materials were high purity Al_2O_3 (99.999 wt.%) and Al_2TiO_5 (99.95 wt.%, with SiO_2 as major impurity). Three different materials were prepared in the Al_2O_3-rich region (20 wt.% Al_2TiO_5, i.e. 11 mol% TiO_2), mid-region (50 wt.% Al_2TiO_5, i.e. 26.4 mol% TiO_2) and eutectic region (43.9 mol% TiO_2) (Fig. 1). These samples will be denoted AT11, AT26 and AT44, respectively. The microstructures were examined on polished sections of the directionally solidified rods using field effect gun–scanning electron microscopy FEG–SEM (LEO Gemini 982). Chemical mappings and profiles were carried out using wavelength dispersive X-ray spectrometry (WDX, CAMECA SX 50). The nanostructures were investigated in transmission electron microscopy using a 200 kV FEG–TEM–STEM (scanning transmission electron microscopy) equipped with an energy dispersive X-ray spectrometer (FEI Tecnai F20).

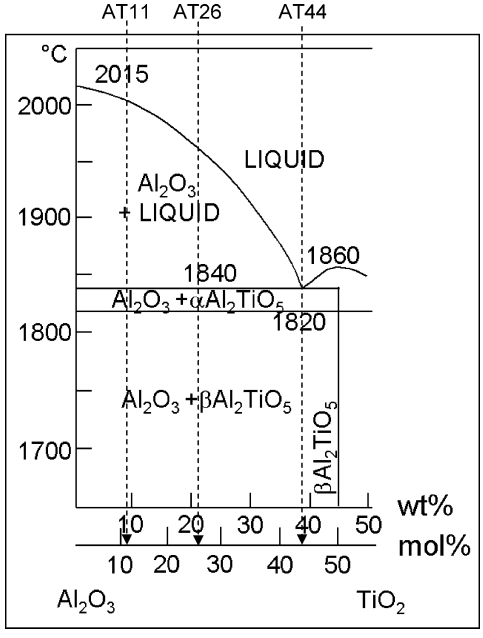

Fig. 1. Al_2O_3-rich side of the phase diagram[14] and solidification path of samples AT11, AT26 and AT44.

3. Results

3.1. Phase identification and distribution in the as-grown rods

3.1.1. Off eutectic compositions (AT11 and AT26)

The samples containing 11 mol% and 26.4 mol% TiO_2 were expected to consist of primary alumina dendrites separated by an Al_2TiO_5/Al_2O_3 eutectic matrix. The SEM observations of Fig. 2a showed well-developed elongated alumina primary dendrites for AT11 and AT26. Their orientations with respect to rod axis could vary in the range of ±30°. WDX chemical analyses Fig. 2c showed that these dendrites were not separated by a two-phase eutectic but by a single-phase aluminum titanate. The composition of this aluminum titanate corresponded to $Al_6Ti_2O_{13}$ (3 mol Al_2O_3 for 2 mol TiO_2) a phase which is not mentioned in the phase diagrams. In addition a thin Al_2TiO_5 interphase (a few 10 nm to 1 μm) was detected by TEM between the alumina dendrites and the $Al_6Ti_2O_{13}$ matrix for the two off eutectic compositions as seen in Fig. 3. Cross-sections showed an average dendrite width of 15 μm and average interdendrite distance of 1.5 μm in AT11 sample whereas for sample AT26 average dendrite width of 30 μm and average interdendrite distance of 30 μm were measured in the central part of the rods.

3.1.2. HRTEM characterization of $Al_6Ti_2O_{13}$ phase

Fig. 4a presents a lattice fringe image exhibiting the three phases: Al_2O_3 dendrite/Al_2TiO_5 interphase/$Al_6Ti_2O_{13}$ matrix in the off eutectic AT26 sample. Fig. 4b exhibits high resolution images of Al_2TiO_5 and $Al_6Ti_2O_{13}$ phases. These images show *b* parameters of the two phases that are similar whereas *c* parameter of $Al_6Ti_2O_{13}$ is ≈5/4 larger than *c* parameter of Al_2TiO_5. Cell parameters of the $Al_6Ti_2O_{13}$, evaluated from SAD patterns and Fourier transforms in [1 0 0] and [0 0 1] zone axes, are listed in Table 2.

Table 2
Evaluation of the cell parameters for $Al_6Ti_2O_{13}$ from SAD and FFT patterns, compared to cell parameters of Al_2TiO_5

	a (Å)	*b* (Å)	*c* (Å)
Al_2TiO_5	3.593	9.439	9.647
$Al_6Ti_2O_{13}$	3.65	9.4	12.4

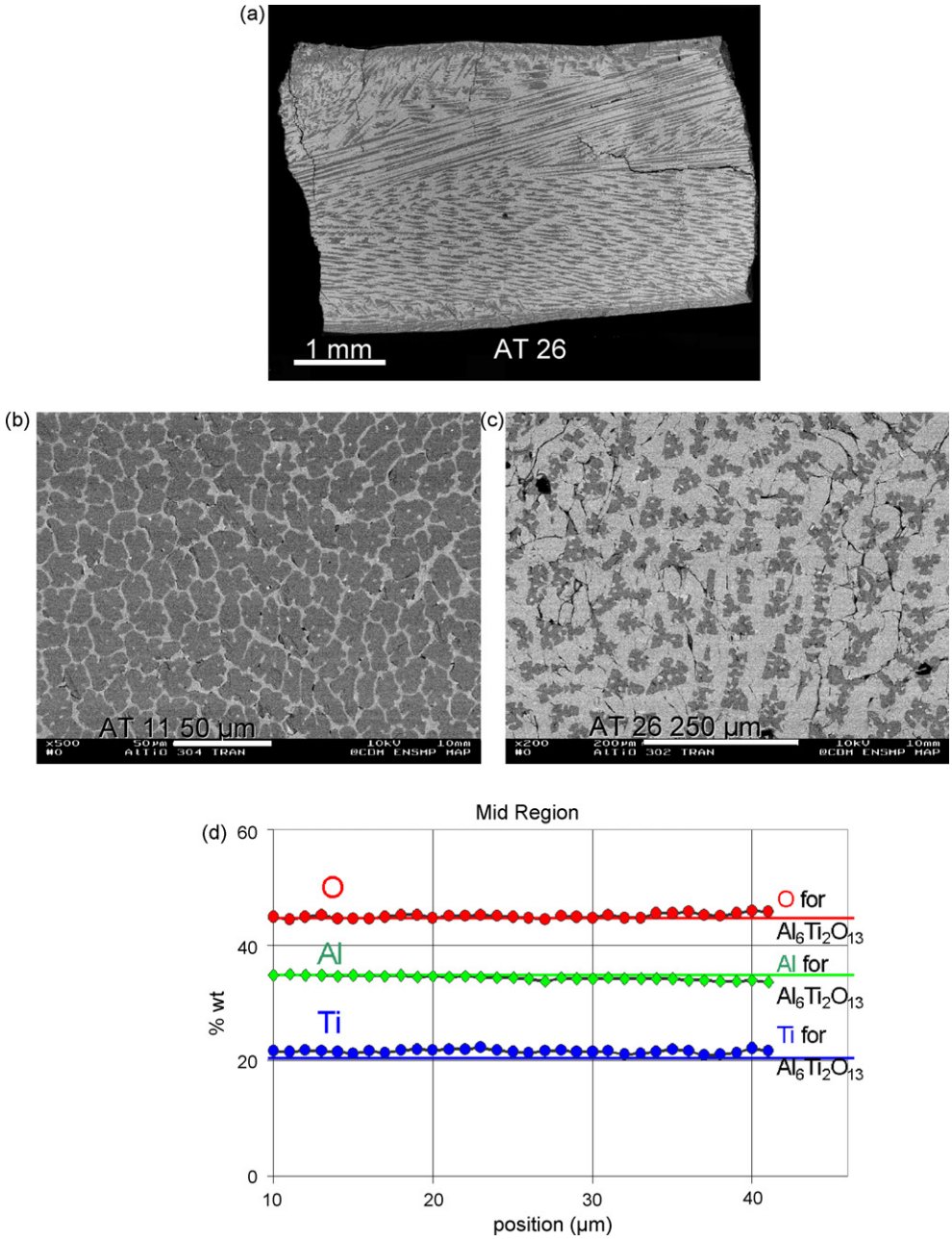

Fig. 2. (a) SEM image of a longitudinal section of sample AT11 exhibiting dark dendrites in a bright matrix. Dentrite growth direction diverge from the rod axis (b) and (c) SEM images of cross-sections of samples AT11 and AT26: distances between dendrites are shorter in the alumina richer sample. (d) WDX profile on sample AT26 on the inter dendrite region: Symbols indicate measurements for O (●), Al (◆) and Ti (●). Horizontal lines correspond to calculated weight percentages in Ti, Al, O for $Al_6Ti_2O_{13}$.

The *a*-, *b*-, and *c*-axes of the two aluminum titanates were systematically aligned and the growth direction was parallel to [1 0 0] for both phases. Simple orientation relationships between aluminum titanates and alumina dendrites were not systematic as the orientation of the dendrites with respect to the growth axis varied contrary to the orientation of aluminum titanates that was kept constant.

3.1.3. Eutectic composition (AT44)

The samples containing 43.9 mol% was expected to consist of a Al_2TiO_5/Al_2O_3 eutectic. SEM observation showed a two-phase lamellar structure, Fig. 5a, but no alumina was detected by WDX analyses. From chemical quantitative chemical profiles, Fig. 5b, it was concluded that the sample enclosed Al_2TiO_5 lamellae in a $Al_6Ti_2O_{13}$ matrix.

3.1.4. $Al_6Ti_2O_{13}/Al_2TiO_5$ intergrowth

High resolution TEM of sample AT44 exhibited Fig. 6a confirmed that the light grey lamellae corresponded to Al_2TiO_5. Contrary to what was concluded from WDX profiles the dark grey matrix was not a $Al_6Ti_2O_{13}$ single phase but was made of a periodic insertion of Al_2TiO_5 single layers between $Al_6Ti_2O_{13}$

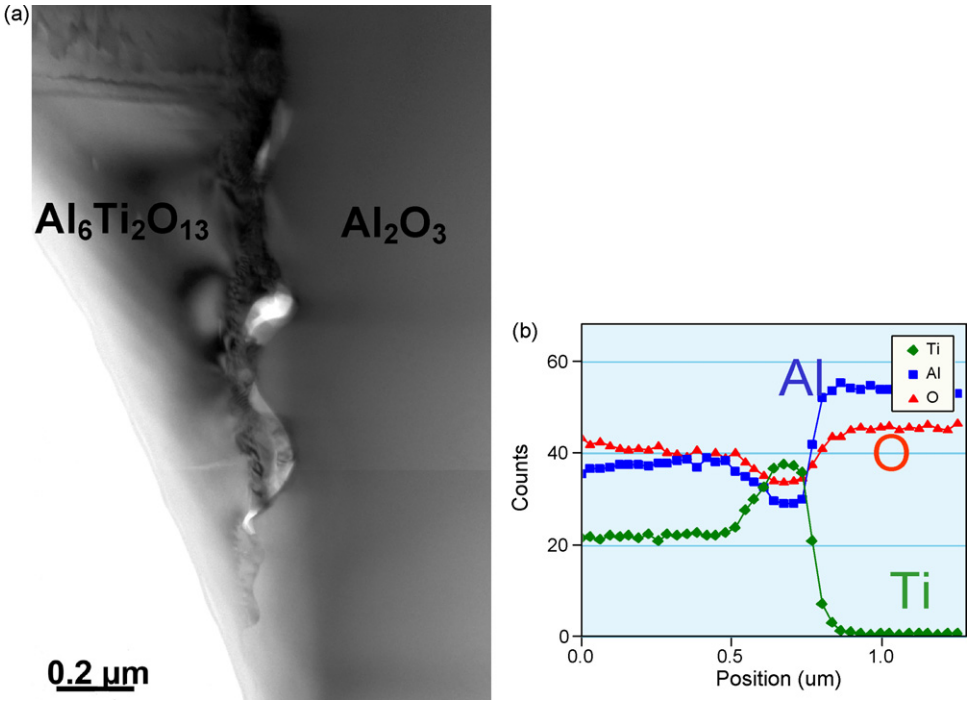

Fig. 3. (a) TEM micrograph showing a Al_2O_3 dendrite edge (left) and the $Al_6Ti_2O_{13}$ phase (left) and an interphase richer in Ti. (b) STEM–EDX profile recorded on across the interface to follow qualitatively the variations of O (●), Al (♦) and Ti (■) in the interphase region.

layers. Fourier transform calculated on the dark grey phase reveals a set of superlattice reflections separated by $\approx 1/7\ nm^{-1}$, Fig. 6b. This frequency corresponds to a mean periodicity of 5 $Al_6Ti_2O_{13}$ layers for 1 Al_2TiO_5 ($5 \times 1.24 + 1 \times 0.96 = 7.16$ nm), although locally 4 layers of $Al_6Ti_2O_{13}$ for one Al_2TiO_5 could also be found as seen in Fig. 6c. The chemical variation induced by a 5:1 intergrowth compared to a $Al_6Ti_2O_{13}$ single phase was less than 0.4 at.% for Al, Ti, and O which is within the WDX atomic resolution for the configuration used in this study and explain why it was not detected by chemical analysis.

The off eutectic samples presented a low degree of insertion of Al_2TiO_5 single layers in the $Al_6Ti_2O_{13}$ matrix. Intergrowth was non-periodic and Al_2TiO_5 single layers were isolated between several tens of $Al_6Ti_2O_{13}$ layers.

3.2. Phase transformation after post-heat treatment

Decomposition of the $Al_6Ti_2O_{13}$ phase was observed for post-heat treatments at 1400 °C for 5 h in air, Fig. 7a. WDX analyses on AT11, AT26 and AT44 samples heat treated at 1500° 10 h showed that $Al_6Ti_2O_{13}$ had totally decomposed into Al_2O_3 and Al_2TiO_5. The AT26 sample consisted of alumina dendrites separated by a composite matrix made of alumina globular grains embedded in Al_2TiO_5, Fig. 7b. The dendrites were surrounded by Al_2TiO_5 layer of few microns almost free of alumina secondary grains. Aluminum cations exsoluted from the $Al_6Ti_2O_{13}$ matrix close from the dendrites could diffuse to the alumina dendrites. In the AT11 sample, Fig. 7c, no alumina secondary grains were observed, interdendritic region contained only Al_2TiO_5. The smaller interdendritic distance in this alumina rich composition allowed the diffusion of all aluminum cations exsoluted from the $Al_6Ti_2O_{13}$ matrix to diffuse to the alumina dendrites. The lamellae structure observed in the as-grown AT44 sample could be recognized in the heat-treated sample, Fig. 7d. The width of the Al_2TiO_5 lamellae increased and they came into contact. Alumina globular grains were aligned in rows parallel to the Al_2TiO_5 phase.

4. Discussion

Directional solidification of a Al-rich Al–Ti–O melt produced an intermediate compound $Al_6Ti_2O_{13}$ which was not reported before on phase diagrams. Melts of compositions AT11 and AT26 produced Al_2O_3 primary dendrites in a $Al_6Ti_2O_{13}$ matrix. This phase is metastable and a post-heat treatment at 1400 °C induced its decomposition by the following eutectoid reaction:

$$Al_6Ti_2O_{13} \rightarrow Al_2O_3 + 2Al_2TiO_5$$

The steep temperature gradients and fast cooling, imposed by laser heated floated zone method, produced conditions for quenching this high temperature aluminum titanate phase.

Eutectoid decomposition occurred on fast cooling only along alumina primary phase of the off eutectic samples and produced a Al_2TiO_5 thin layer around the alumina dendrites. These dendrites provided energetically favourable sites for the exsolution of Al_2O_3 from the $Al_6Ti_2O_{13}$.

Solidification of composition AT44, which was referred as "eutectic" based on phase diagram, produced $Al_6Ti_2O_{13}$ and Al_2TiO_5 but no alumina. This indicates that eutectoid reaction did not occur on fast cooling. The absence of Al_2O_3 seeds that could lower energy barrier for the eutectoid decomposition of

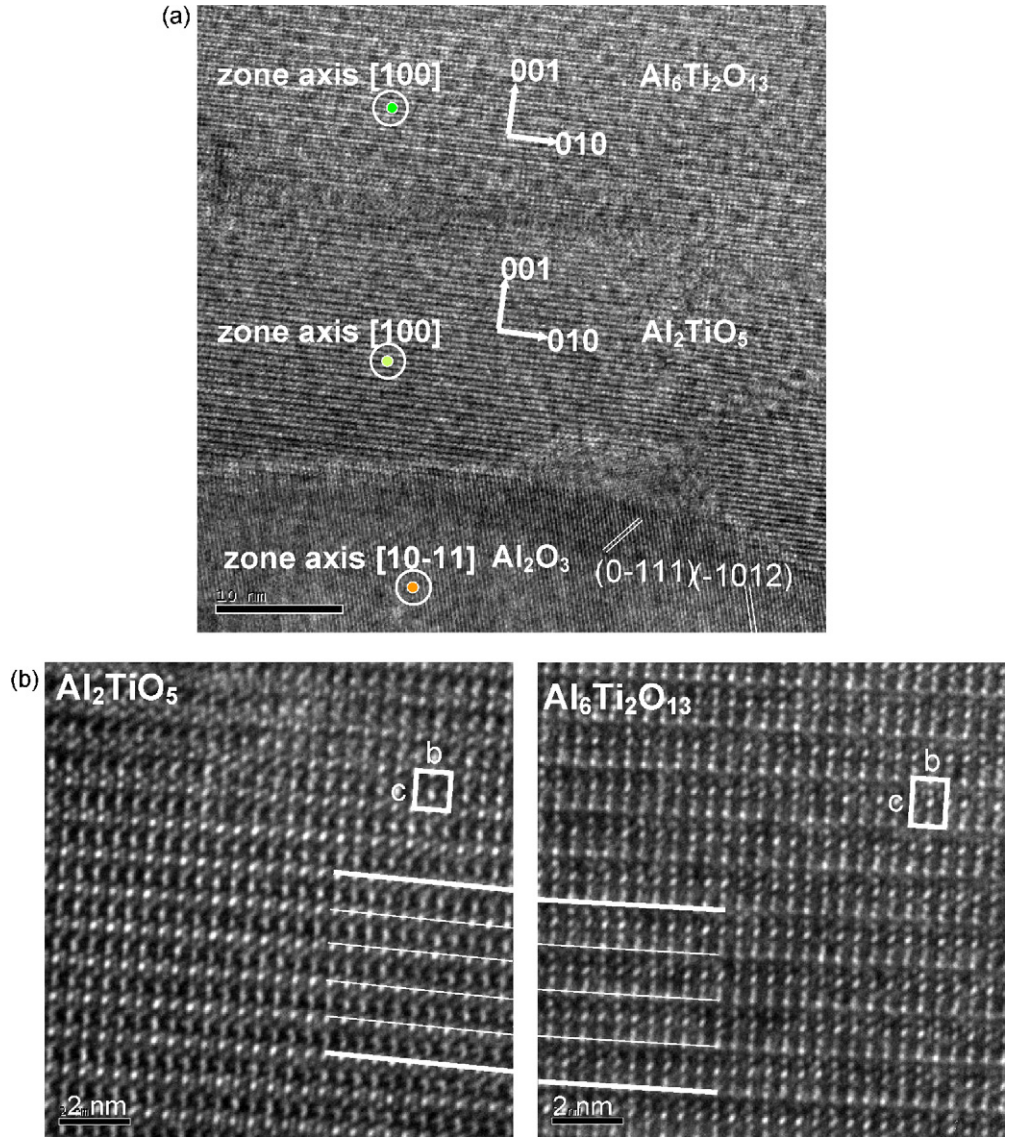

Fig. 4. (a) $Al_6Ti_2O_{13}/Al_2TiO_5/Al_2O_3$ region in sample AT26 and corresponding. Aluminum titanates are in [1 0 0] zone axis and alumina in[10,11] zone axis. Interfaces are curved and not observed edge on. (b) High resolution TEM images Al_2TiO_5 (left) and $Al_6Ti_2O_{13}$ (right) both in [1 0 0] zone axis. Solid lines illustrate the relation $5d_{0\,0\,1,Al_2TiO_5} \approx 4d_{0\,0\,1,Al_6Ti_2O_{13}}$.

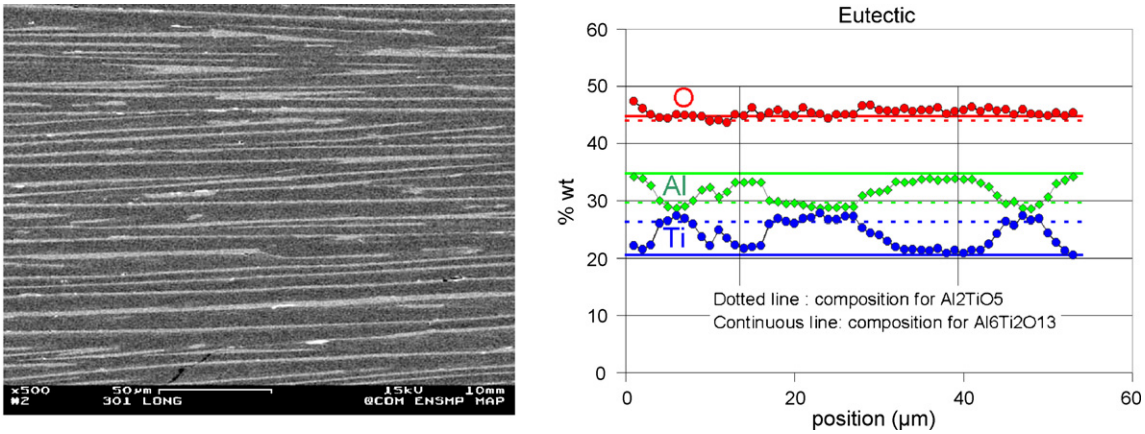

Fig. 5. Sample AT44 (43.9 mol% TiO_2): (a) SEM image of a longitudinal section exhibiting continuous bright lamellae in a dark matrix, (b) WDX profile along a diagonal line with respect to the growth axis. Symbols indicate measurements for O (●), Al (♦) and Ti (■). Horizontal lines correspond to calculated weight percentages in Ti, Al, O for $Al_6Ti_2O_{13}$ (solid lines, dark phase) and for Al_2TiO_5 (dotted lines, light phase).

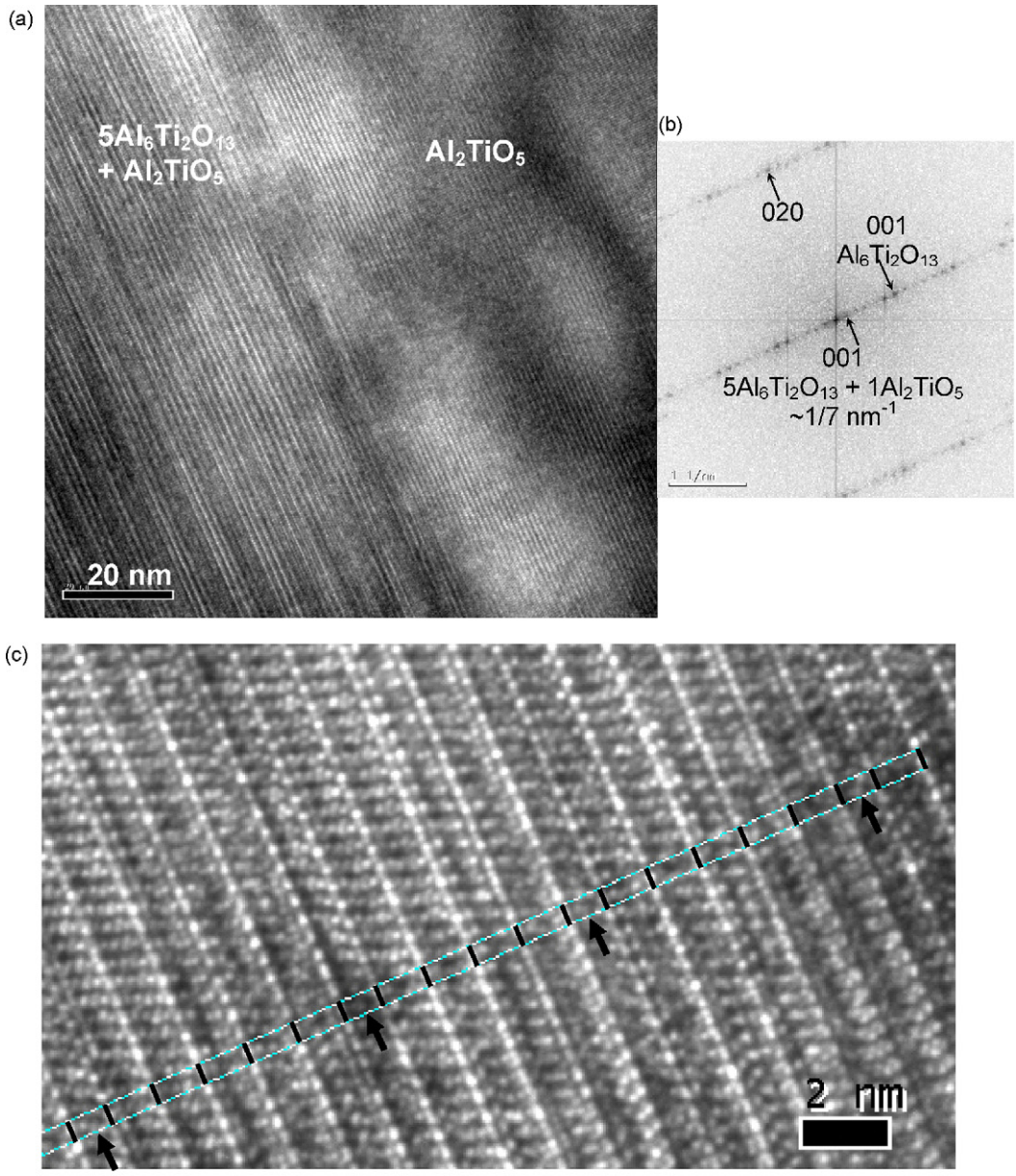

Fig. 6. (a) Interface region between lamella (right) and matrix (left) in sample AT44 observed in [1 0 0] zone axis (growth axis), (b) FTT of the matrix region. The FFT shows superlattice reflections at 1/7 nm^{-1} corresponding to a mean periodicity of one block Al_2TiO_5 inserted every five blocks of $Al_6Ti_2O_{13}$. (c) Detail of the matrix region showing one Al_2TiO_5 block (black arrow) every five or four blocks of $Al_6Ti_2O_{13}$.

$Al_6Ti_2O_{13}$, explain the difference with the off eutectic compositions.

Goldberg[16] in 1968 reported the formation of metastable alumina rich aluminum titanates. Later Mazerolles et al. described intergrowth between Al_2TiO_5 and these alumina richer phases[17]. But exact compositions were not published by Goldberg or Mazerolles. Göbbels and Bostroem published an extended abstract[18] describing the solidification of $Al_6Ti_2O_{13}$ and proposed a first structure for this new phase. The $Al_6Ti_2O_{13}$ structure was derived from the Al_2TiO_5 pseudo brookite structure. This later structure is made of the double chains running along the *c*-direction, built by groups of three distorted octahedra. The $Al_6Ti_2O_{13}$ structure was obtained by the insertion of an additional octahedron in each group of three distorted octahedra. One of these additional octahedra was occupied randomly by Ti^{4+} or Al^{3+} whereas the second octahedron of the double chain was only occupied by Al^{3+}. The authors did not confirm further their structure in a full article. Distances between Al^{3+} and O^{2-} for the second additional polyhedron were not compatible with octahedron coordination. Attempts at determination of atomic arrangement was also carried out by Mazerolles[19] with similar difficulties as Göbbels. Recently Norberg et al.[20] proposed a refined structure for $Al_6Ti_2O_{13}$. These authors indicated an orthorhombic structure, space group, *Cm2m*, with cell

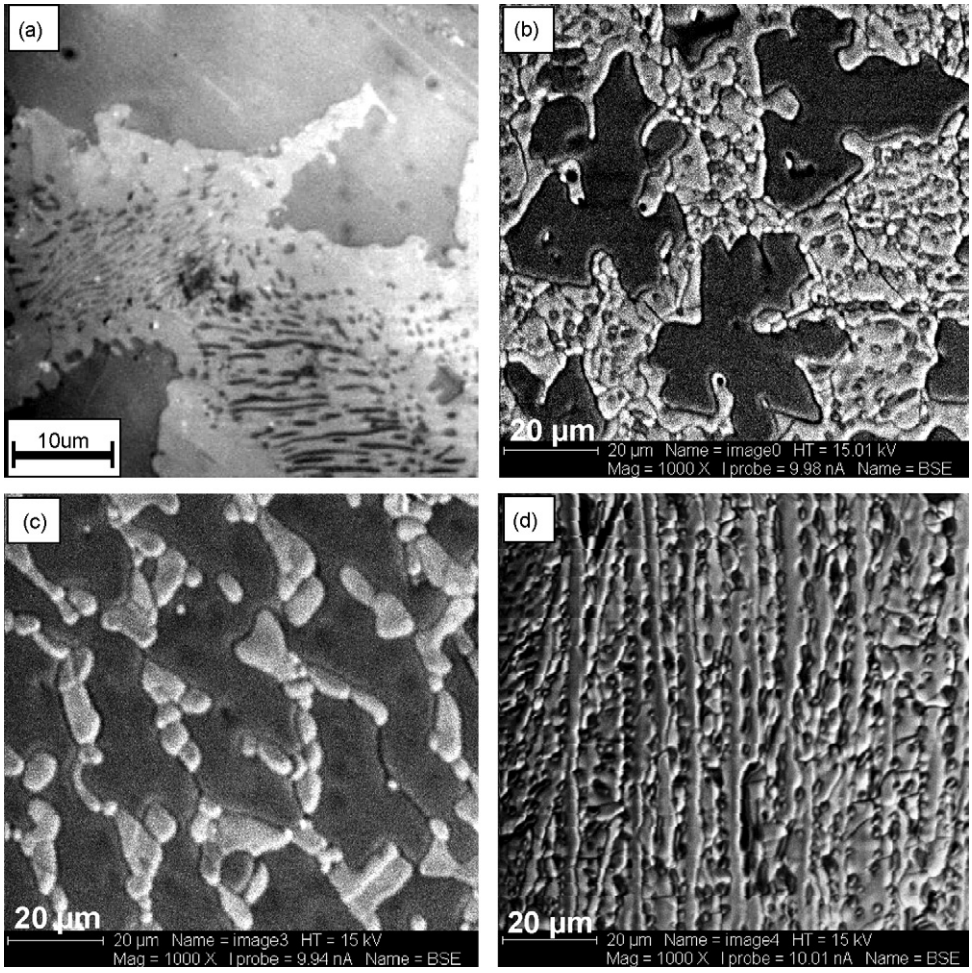

Fig. 7. (a) Optical image of sample AT26 annealed for 5 h at 1400 °C: eutectoid reaction occurred in the $Al_6Ti_2O_{13}$ matrix to form Al_2TiO_5 matrix (light grey) and Al_2O_3 precipitates (dark grey) a few micron apart from the primary dendrites. (b)–(d) SEM images of the three compositions annealed for 10 h at 1500 °C. The samples consist of Al_2O_3 (darker phase) and Al_2TiO_5 (brighter phase). (b) AT11: Al_2TiO_5 grains between Al_2O_3 dendrites. (c) AT26: Al_2O_3 dendrites, Al_2O_3 precipitates included in Al_2TiO_5 phase. (d) AT44: Al_2TiO_5 lamellae in contact to each other, precipitates of Al_2O_3 aligned in rows parallel to the Al_2TiO_5.

parameters $a = 3.65$ Å, $b = 9.368$ Å, $c = 12.555$ Å. The structure consists of infinite double chains of polyhedra running along the c axis. These chains are built up by four oxygen octahedra, strongly distorted and randomly occupied by either Ti or Al, as in the structure suggested by Goebbels et al. These two structures differed only in the additional sites that are occupied by aluminum cations. The octahedron in the structure proposed by Goebbels et al. was replaced by a trigonal bipyramid in the structure recently proposed by Norberg et al.

The similitude of the $Al_6Ti_2O_{13}$ and Al_2TiO_5 structure with very close a and b parameters explains the systematic identical orientation of the cells across $Al_6Ti_2O_{13}/Al_2TiO_5$ interfaces and the low interface energy along (0 0 1) that favours intergrowth.

The present work confirms the existence of a second compound between Al_2O_3 and TiO_2 that has been studied by Goldberg, Mazerolles, Goebbels, and Norberg. The work of Goldberg,[16] questioning the alumina rich part of this Al_2O_3–TiO_2 phase diagram has therefore to be pursued. The authors of the present article do not have the ambition to establish a new phase diagram. Main objections for this, is that equilibrium conditions were not reached during solidification and exact temperatures of solidification or eutectoid reaction were not measured. However the phase distributions established for the samples at 11, 26 and 43.9 mol% TiO_2 permit to propose directions for a future modification of this diagram.

Previously published phase diagrams present a Al_2TiO_5 intermediate compound at 50 mol% TiO_2. The sharp minimum in the liquidus temperature at around 43.9 mol% TiO_2, first measured by Bunting,[12] was always interpreted as an invariant eutectic point between Al_2TiO_5 and Al_2O_3. However no microstructures showing evidence of a Al_2TiO_5/Al_2O_3 eutectic at 43.9 mol% TiO_2 (or 38.5 wt.% TiO_2) were found in the literature. On the contrary, Rowcliff et al.[21] describe samples grown at the "eutectic" composition with these words: "evidently these samples were not of the eutectic composition which probably contain more titania than 38.5 wt.%".

The phase diagram published by Lang et al.[13] attracted our attention for two reasons. First the diagram shows the formation of a high temperature form of Al_2TiO_5 called α-Al_2TiO_5 that decomposes into β-Al_2TiO_5 at 1820 °C. This allotropic high temperature form of Al_2TiO_5 was not characterized because it could never be quenched. Second, they propose two versions of their phase diagram with distinct invariant points: one with a eutectic point ($L \rightarrow Al_2TiO_5 + Al_2O_3$), the other with a peritec-

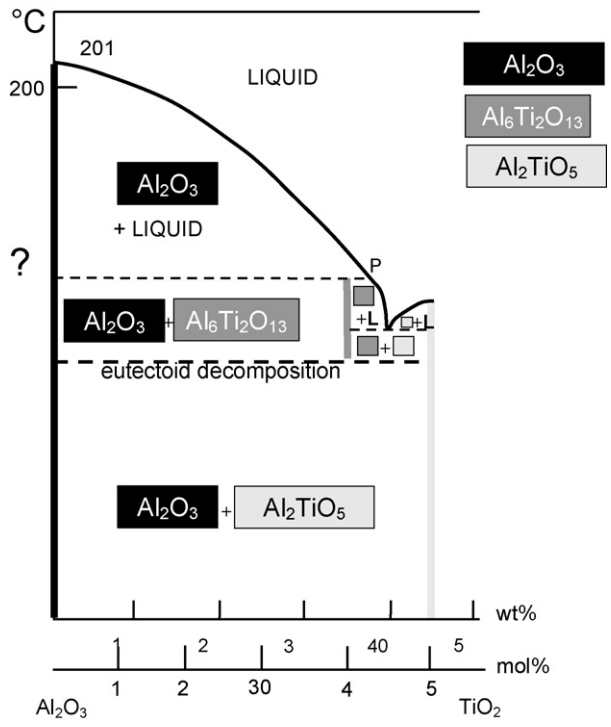

Fig. 8. Suggested outlines for Al_2O_3-rich part of the Al_2O_3–TiO_2 phase diagram.

tic point ($L + Al_2O_3 \rightarrow Al_2TiO_5$). From our observations, we suggest that the high temperature phase was not an allotropic form of Al_2TiO_5 but $Al_6Ti_2O_{13}$ and that both eutectic (*E*) and peritectic (*P*) points coexist, but with the following reactions: *E*: $L \rightarrow Al_2TiO_5 + Al_6Ti_2O_{13}$ and *P*: $L + Al_2O_3 \rightarrow Al_6Ti_2O_{13}$ as will be explained below.

A vertical segment at 40 mol% is added on this outline of phase diagram of Fig. 8 which represents the high temperature $Al_6Ti_2O_{13}$ phase. The introduction of this new compound induces the insertion of an invariant point on the liquidus, that can be either a eutectic point ($L \rightarrow Al_6Ti_2O_{13} + Al_2O_3$) at less than 40 mol% TiO_2 or a peritectic point ($L + Al_2O_3 \rightarrow Al_6Ti_2O_{13}$) at more than 40 mol% of TiO_2. No Al_2O_3 domains were observed by TEM and HRTEM in the $Al_6Ti_2O_{13}$ interdendritic region for samples AT11 and AT26 that could support the hypothesis of a $Al_6Ti_2O_{13}$–Al_2O_3 eutectic. The hypothesis of a peritectic reaction involves a liquid, richer in titania than $Al_6Ti_2O_{13}$, in contact with solid Al_2O_3. Titanium and oxygen ions from the liquid react with alumina and a $Al_6Ti_2O_{13}$ solid layer is formed at the liquid/solid interface. The further consummation of the excess Ti cations in the liquid to attain a melt of $Al_6Ti_2O_{13}$ molar composition requires diffusion of the excess ions through the interfacial reaction layer to reach alumina. The fast solidification rates used in this work might be kinetically incompatible with a total consummation of the excess Ti cations by solid diffusion. The HRTEM observations of sample AT26 have revealed a small level of intergrowth of Al_2TiO_5 between $Al_6Ti_2O_{13}$. This intergrowth demonstrates that solidification of a liquid richer in titania than $Al_6Ti_2O_{13}$ formed. The chemical shift was balanced by the intergrowth of Al_2TiO_5, phase richer in titania than $Al_6Ti_2O_{13}$. The high-degree of resemblance between Al_2TiO_5 and Al_2TiO_5 structures render this intergrowth as energetically favourable. The low density of intergrowth in AT26 matrix supports a peritectic point close to $Al_6Ti_2O_{13}$.

The sharp minimum in the liquidus temperature at around 43.9 mol% TiO_2, which was first measured by Bunting[12] was previously interpreted as an invariant eutectic point between Al_2TiO_5 and Al_2O_3. The insertion of the $Al_6Ti_2O_{13}$ compound in the phase diagram between Al_2TiO_5 and Al_2O_3 modifies the constituent phases of the eutectic region, which must be formed between $Al_6Ti_2O_{13}$ and Al_2TiO_5. This suggestion is further supported by the structural analysis of sample solidified from a melt with 43.9 mol% TiO_2 composition. The rapid solidification did not produce Al_2O_3 and Al_2TiO_5. Lamellae of Al_2TiO_5 were separated by an aluminum titanate superstructure formed by an intergrowth between $Al_6Ti_2O_{13}$ and Al_2TiO_5. The average composition of this superstructure was very close to that of $Al_6Ti_2O_{13}$. It is likely that the composition of sample 43.9 mol% TiO_2 was not strictly that of the $Al_6Ti_2O_{13}$–Al_2TiO_5 eutectic but slightly richer in TiO_2. The eutectic invariant point has been placed around 43.5 mol% TiO_2. The high viscosity of the melt and its tendency to supercool during fast solidification does not permit to fix the eutectic composition precisely.

5. Conclusions

Directional solidification characteristics of Al_2O_3–TiO_2 melts with 11, 26, 43.9 mol% of TiO_2 content were investigated using laser heated float zone method. Based on microstructural characterization using XRD, WDX, SEM, HRTEM and STEM–EDX analyses we had the following conclusions.

- No Al_2O_3–Al_2TiO_5 eutectic was formed for any compositions studied. This is in contradiction with previous phase diagrams that suggest formation of Al_2O_3–Al_2TiO_5 eutectic for 43.9 mol% TiO_2 and formation of primary Al_2O_3 dendrites separated by Al_2O_3–Al_2TiO_5 eutectic for off eutectic compositions, 11 and 26 mol% TiO_2.
- An additional phase $Al_6Ti_2O_{13}$ crystallized that was not previously predicted by the phase diagrams. The $Al_6Ti_2O_{13}$ phase has *a* and *b* parameters analogous to that of Al_2TiO_5 and *c* was equal to ~5/4 that of Al_2TiO_5. Alignment of the $Al_6Ti_2O_{13}$ and Al_2TiO_5 cell base vectors was systematically observed.
- The solidification of the 11 and 26 mol% TiO_2 melt produced alumina primary dendrites separated by $Al_6Ti_2O_{13}$ matrix. An Al_2TiO_5 interphase was formed during fast cooling between $Al_6Ti_2O_{13}$ and Al_2O_3 from the $Al_6Ti_2O_{13}$ matrix. The solidification of the 43.9 mol% TiO_2 produced a lamellae structure composed of Al_2TiO_5 and an aluminum titanate superstructure that consist of intergrowth in the [0 0 1] direction (one Al_2TiO_5 cell for five $Al_6Ti_2O_{13}$ cells).
- Post-heat treatment at 1400 °C decomposed $Al_6Ti_2O_{13}$ into Al_2O_3 and Al_2TiO_5 by a eutectoid reaction. This solid-state reaction could not take place during laser processing of the materials due to the rapid cooling rates, except locally around

alumina dendrites, which offered energetically favourable nucleation sites for the decomposition.

- Based on these observations an outline of a new phase diagram was proposed for the Al_2O_3-rich side of Al_2O_3–TiO_2 system. A line compound $Al_6Ti_2O_{13}$ is added as a high temperature phase at 40 mol% TiO_2 which defined new phase fields at high temperatures. The eutectic invariant point is at ~43.5% TiO_2 between $Al_6Ti_2O_{13}$ and Al_2TiO_5 phases. A peritectic point was suggested between $Al_6Ti_2O_{13}$ and the $Al_6Ti_2O_{13}$–Al_2TiO_5 eutectic.

Acknowledgements

This research was funded by NASA cooperative agreement NNC04 AA27A and through European Office of Aerospace Research and Development by AFOSR under Grant No. FA8655-03-1-3040. The authors would like to thank Gérard Frot of Mines de Paris who performed the WDX analyses of this study.

References

1. Sayir, A., Directionally solidified eutectic ceramics. In *Computer-aided Design of High-temperature Materials*, ed. A. Pechenik, R. K. Kalia and P. Vashista. Oxford University Press, 1999, pp. 197–211.
2. Stubican, V. S. and Brandt, R. C., Eutectic solidification in ceramic systems. *Ann. Rev. Mater. Sci.*, 1981, **11**, 267–297.
3. LLorca, J. and Orera, V., Directionally solidified eutectic ceramic oxides. *Prog. Mater. Sci.*, 2006, **51**, 711–809.
4. Sayir, A. and Farmer, S. C., The effect of the microstructure on mechanical properties of directionally solidified Al_2O_3/ZrO_2 (Y_2O_3) eutectic. *Acta Mater.*, 2000, **48**, 4691–4697.
5. Parthasarathy, T. A., Mah, T. and Matson, L. E., Deformation behaviour of an Al_2O_3–$Y_3Al_5O_{12}$ eutectic composite in comparison with sapphire and YAG. *J. Am. Ceram. Soc.*, 1993, **76**(1), 29–32.
6. Argon, A. S., Yi, J. and Sayir, A., Creep resistance of directionally solidified ceramic eutectics of Al_2O_3/C–ZrO_2 with sub-micron columnar morphologies. *Mater. Sci. Eng.*, 2001, **A319–321**, 838–842.
7. Matson, L. E., Hay, R. S. and Mah, T., Stability of a sapphire/yttrium aluminum garnet composite system. *Ceram. Eng. Sci. Proc.*, 1989, **10**, 764.
8. Waku, Y., Nakagawa, N., Wakamoto, T., Ohtsubo, H., Shimizu, K. and Kohtoku, Y., High-temperature strength and thermal stability of a unidirectionally solidified Al_2O_3/YAG eutectic composite. *J. Mater. Sci.*, 1998, **33**, 1217–1225.
9. Thomas, H. A. J. and Stevens, R., Aluminium titanate—a literature review. Part I: Microcraking phenomena. *Br. Ceram. Trans. J.*, 1989, **88**, 144–151.
10. Bueno, S., Moreno, R. and Baudín, C., Reaction sintered Al_2O_3/Al_2TiO_5 microcrack-free composites obtained by colloidal filtration. *J. Eur. Ceram. Soc.*, 2004, **24**(9), 2785–2791.
11. Von Wartenburg, H. and Reusch, H. J., Melting diagrams of heavy duty oxides IV (aluminium oxide). *Zeit. Anorg. Allgem. Chem.*, 1932, **207**, 1.
12. Bunting, E. N., Phase equilibria in the systems TiO_2, TiO_2–SiO_2 and TiO_2–Al_2O_3. *Bur. Stand. J. Res.*, 1933, **11**, 725.
13. Lang, S. M., Fillimore, C. L. and Maxwell F L.H., The system beryllia–alumina–titania: phase relations and general physical properties of three-component porcelains. *Res. Natl. Bur. Stand.*, 1952, **48**, 298.
14. Sayir, A., Berger, M. H. and Baudín, C., Microstructural and mechanical properties of directionally solidified ceramic in Al_2O_3–Al_2TiO_5 system. *Ceram. Eng. Sci. Proc.*, 2005, **26**(2), 225–233.
15. Baudín, C., Sayir, A. and Berger, M. H., Mechanical behavior of directionally solidified alumina/aluminum titanate ceramics. *Acta Mater.*, 2006, **54**(14), 3835–3841.
16. Goldberg, D., Contribution à l'étude des systèmes formés par l'alumine avec quelques oxydes de métaux trivalents ,et tétravalents, en particulier l'oxyde de titane. *Rev. Int. Hautes Tempér. et Réfract.*, 1968, **5**, 181–194.
17. Mazerolles, L., Bianchi, V. and Michel, D., Intergrowth between pseudobrookite and related phases. In *Proceedings of ICEM 13*, 1994, pp. 905–906.
18. Goebbels, M. and Bostroem, D., Kristallzüchtung und Struktur von $Al_6Ti_2O_{13}$. *Berichter der Deutschen Mineralogishen Gesellshaft*, 1997, **9**(1), 128.
19. Mazerolles, L., private communication.
20. Norberg, S. T., Hoffmann, S., Yoshimura, M. and Ishizawa, N., $Al_6Ti_2O_{13}$, a new phase in the Al_2TiO_2 system. *Acta Cryst.*, 2005, **C61**, i35–i38.
21. Rowcliff, D. J., Warren, W. J., Elliot, A. G. and Rothwell, W. S., The growth of oriented ceramic eutectics. *J. Mater. Sci.*, 1969, **4**, 902–907.